Chinese Chemical Letters 32 (2021) 3387–3392

Contents lists available at ScienceDirect

Chinese Chemical Letters

journal homepage: www.elsevier.com/locate/cclet

Communication

Ferric ion-ascorbic acid complex catalyzed calcium peroxide for organic wastewater treatment: Optimized by response surface method

Deling Yuan[a,b], Chen Zhang[a], Shoufeng Tang[a,b,*], Zetao Wang[a], Qina Sun[a], Xiaoyu Zhang[a], Tifeng Jiao[a,b,*], Qingrui Zhang[a,b]

[a] Hebei Key Laboratory of Heavy Metal Deep-Remediation in Water and Resource Reuse, Hebei Key Laboratory of Applied Chemistry, School of Environmental and Chemical Engineering, Yanshan University, Qinhuangdao 066004, China
[b] State Key Laboratory of Metastable Materials Science and Technology, Yanshan University, Qinhuangdao 066004, China

ARTICLE INFO

Article history:
Received 30 January 2021
Revised 15 April 2021
Accepted 27 April 2021
Available online 4 May 2021

Keywords:
Ferric ion
Ascorbic acid
Calcium peroxide
Response surface method
Dye removal

ABSTRACT

Hydrogen peroxide (H_2O_2) disproportionation, iron precipitation, and narrow pH range are the drawbacks of traditional Fenton process. To surmount these barriers, we proposed a ferric ion (Fe^{3+})-ascorbic acid (AA) complex catalyzed calcium peroxide (CaO_2) Fenton-like system to remove organic dyes in water. This collaborative Fe^{3+}/AA/CaO_2 system presented an obvious improvement in the methyl orange (MO) decolorization, and also effectively eliminated other dyes. Response surface method was employed to optimize the running parameters for this coupling process. Under the optimized arguments (2.76 mmol/L Fe^{3+}, 0.68 mmol/L AA, and 4 mmol/L CaO_2), the MO removal achieved 98.90% after 15 min at pH 6.50, which was close to the computed outcome of 99.30%. Furthermore, this Fenton-like system could perform well in a wide range of pH (3–11), and enhance the H_2O_2 decomposition and Fe ions recycle. The scavenger experiment result indicated that hydroxyl radical, superoxide anion free radical, and singlet oxygen were acted on the dye elimination. Moreover, electron spin resonance analysis corroborated that the existences of these active species in the Fe^{3+}/AA/CaO_2 system. This study could advance the development of Fenton-like technique in organic effluent disposal.

With the development of industrialization, the traditional physical, biological and chemical methods cannot meet the requirements of efficient wastewater treatment of refractory organics [1–3]. Advanced oxidation processes (AOPs) are expected to reach high requirements and strict regulations in organic effluent disposal [4]. AOPs include photocatalysis [5–7], catalytic ozonation [8], catalytic wet air oxidation [9,10], electrochemical oxidation [11,12], and Fenton reaction [13,14]. One of the most widely used is Fenton oxidation, that is, ferrous ion (Fe^{2+}) activates hydrogen peroxide (H_2O_2) to produce hydroxyl radical (•OH) [15]. The •OH has high oxidation ability, which can quickly and non-selectively degrade various refractory organics in water [16].

Fenton system has some of the advantages, such as mild reaction conditions, simple equipment, convenient operation, and high oxidation rate [17]. However, the pH range of Fenton reaction is narrow (pH 3–5) [18]. H_2O_2 is easy to be decomposed, leading to the decrease of utilization [19]. Besides, the liquid H_2O_2 is inconvenient for storage and transportation. Moreover, Fe^{2+} is hard to recover and liable to produce the precipitation of ferric ion (Fe^{3+}) [20]. These factors limit the Fenton reaction efficiency and its further application.

To overcome the bottlenecks of conventional Fenton reaction, the improved Fenton and Fenton-like processes have been well developed recently [21]. Introducing complexing agent into Fenton reaction is the most common way, which can effectively prolong the existence time of dissolved Fe^{2+} and Fe^{3+}, broaden the appli-

* Corresponding authors at: Hebei Key Laboratory of Heavy Metal Deep-Remediation in Water and Resource Reuse, Hebei Key Laboratory of Applied Chemistry, School of Environmental and Chemical Engineering, Yanshan University, Qinhuangdao 066004, China.
E-mail addresses: tangshf@ysu.edu.cn (S. Tang), tfjiao@ysu.edu.cn (T. Jiao).

https://doi.org/10.1016/j.cclet.2021.04.050
1001-8417/

cation range of pH value, promote electron transfer, and prevent iron precipitation [22]. The usual chelation agents are ethylenediaminetetraacetic acid and hydroxylamine, but they would generate toxic products during reactions and secondary pollution [23–25]. So diverse small molecule organic acids have attracted great attention, such as ascorbic acid (AA) [26], citric acid [27] and oxalic acid [28]. These carboxylates could not only have the favorable complexing capability, but also be nontoxic and degradable.

Calcium peroxide (CaO_2) is a stable solid peroxide, which is easy to transport and store. CaO_2 could slowly and stably produce H_2O_2 over a broad range of pH, reducing the disproportionation of H_2O_2. Hence, CaO_2 has been extensively researched as the substitution of H_2O_2 [29]. On the other side, Fe^{3+} is more stable than Fe^{2+}, and Fe^{3+} could also catalyze H_2O_2 by initiative superoxide and per hydroxyl actuated reactions to generate a series of reactive oxygen species [30], such as $^{\bullet}OH$ and superoxide anion free radical ($O_2^{\bullet-}$). But the direct application of Fe^{3+} would easily form iron sludge, exhausting the Fenton reactivity. Also, the reduction of Fe^{3+} to Fe^{2+} is slowly.

To sum up, using the AA complexed Fe^{3+} to react with CaO_2 is a prospective improved method to surmount the application barriers of traditional Fenton reaction, which is seldom reported. In addition, response surface method (RSM) combines math and statistics means to model and optimize the influence of a few independent variables, which is widely and efficiently applied for the modelling and optimization in the various engineering issues. Therefore, we established a Fe^{3+}-AA complex catalyzed CaO_2 (Fe^{3+}/AA/CaO_2) Fenton-like process to promote the removal of multiple organic dyes in water, and the operation parameters (Fe^{3+} concentration, AA dosage, and CaO_2 amount) were optimized by the RSM for the methyl orange (MO) decolorization. Furthermore, the H_2O_2 decomposition, Fe ions change, and active species identification were studied to reveal the synergistic reaction mechanisms.

The sources properties of chemicals applied in this study were introduced in Text S1 (Supporting Information). The tests were implemented in flask (100 mL) at room temperature on magnetic stir. The desired concertation of simulated wastewater was added in the beaker, and its initial pH was regulated by sulfuric acid and sodium hydroxide. Then, the reaction was initiated through adding Fe^{3+}, AA, and CaO_2 in order. Sample aliquots (1 mL) was extracted at the given time intervals, and added 1 mL sodium thiosulfate to quench oxidation process, then filtered by 0.22 μm filter membrane for determination of concentration. The dye concentration was measured by the UV-spectrophotometer at different specific wavenumbers. The total organic carbon (TOC) was monitored through TOC analysis meter. The H_2O_2 amount was determined by titanium potassium oxalate method [31]. The concentrations of Fe^{3+} and total Fe were detected by 1,10-phenanthroline monohydrate color method [32]. The determination of Fe^{4+} was used by dimethyl sulfoxide (DMSO) oxidation method [33]. *Tert*-butyl alcohol (TBA), *p*-benzoquinone (BQ) and L-histidine were used to quench $^{\bullet}OH$, $O_2^{\bullet-}$, and singlet oxygen ($^1O_2$), respectively. The qualitative test for active species was determined through electron spin resonance (ESR) spectrometer. The detailed analyses parameters were described in Text S2 (Supporting information).

The RSM from Box-Behnken was designed on the basis of Design-Expert 8.0.6 Trial software. The experimental design of three factors (Fe^{3+} dose, AA concentration, and CaO_2 amount) and three levels was adopted to investigate the MO removal. The detailed design and analysis of RSM described in Text S3 (Supporting information), and the numbered and actual values for the variables were presented in Table S1 (Supporting information).

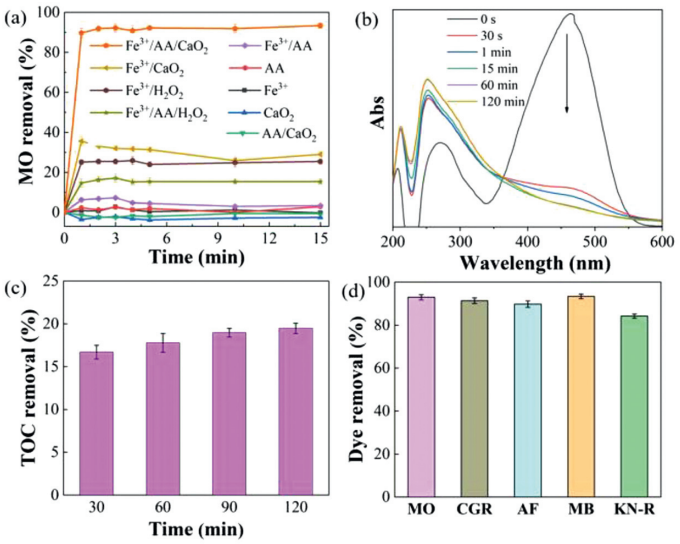

Fig. 1. (a) MO removal in different processes. (b) UV–vis spectroscopy for MO decolorization. (c) TOC removal of MO. (d) Different dyes removal in Fe^{3+}/AA/CaO_2 system. Conditions: [MO] = [other dyes] = 0.15 mmol/L, [Fe^{3+}] = 2 mmol/L, [AA] = 1 mmol/L, [CaO_2] = [H_2O_2] = 3 mmol/L, initial pH 6.50.

Fig. 1a compares the MO removal by the Fe^{3+}/AA/CaO_2 and other control processes. There were no MO decolorization by the Fe^{3+} alone, AA alone, CaO_2 alone, AA/CaO_2, and Fe^{3+}/AA systems, and only 28.90% of MO was decolored in the Fe^{3+}/CaO_2 after 15 min treatment. Nevertheless, 93.40% of MO was removed by the Fe^{3+}/AA/CaO_2, indicating the significant improvement in the synergistic process. In contrast, the MO removals were 25.40% and 15.30% for the Fe^{3+}/H_2O_2 and Fe^{3+}/AA/H_2O_2, respectively, which was clearly inferior to the CaO_2 relevant processes. Above phenomena could be explained through the following reasons: firstly, the dissolved CaO_2 could stably supply H_2O_2 for the Fenton-like system and release O_2 simultaneously (R1 and R2) [34], avoiding the disproportionation of H_2O_2. Secondly, after adding the AA, the complexation of Fe^{3+} and AA could be formed (R3) [34,35], which could accelerate the electron transfer, improving the Fe^{2+} formation from the Fe^{3+} reduction and decreasing the precipitation of Fe^{3+}. Thirdly, except for the conventional Fenton reactions for the generations of $^{\bullet}OH$ and $O_2^{\bullet-}$ (R4 and R5), the AA mediated Fe^{3+}/CaO_2 process could produce more reactive species, such as $O_2^{\bullet-}$ and $^1O_2$ (R6 and R7) [36,37], which are the more selective species for oxidizing the electron-rich groups in the organic compounds.

$$CaO_2 + H_2O \rightarrow H_2O_2 + Ca(OH)_2 \quad (1)$$

$$CaO_2 + H_2O \rightarrow 0.5O_2 + Ca(OH)_2 \quad (2)$$

$$2Fe^{3+} + AA \rightarrow Fe^{2+}/Fe^{3+}\text{-}AA \rightarrow 2Fe^{2+} \quad (3)$$

$$Fe^{2+} + H_2O_2 \rightarrow Fe^{3+} + OH^- + {}^{\bullet}OH \quad (4)$$

$$Fe^{3+} + H_2O_2 \rightarrow Fe^{2+} + H^+ + HO_2^{\bullet} \quad (5)$$

$$Fe^{2+}/Fe^{3+}\text{-}AA + HO_2^{\bullet} \rightarrow Fe^{2+}/Fe^{3+}\text{-}AA + H^+ + O_2^{\bullet-} \quad (6)$$

$$2O_2^{\bullet-} + 2H_2O \rightarrow H_2O_2 + {}^1O_2 + 2OH^- \quad (7)$$

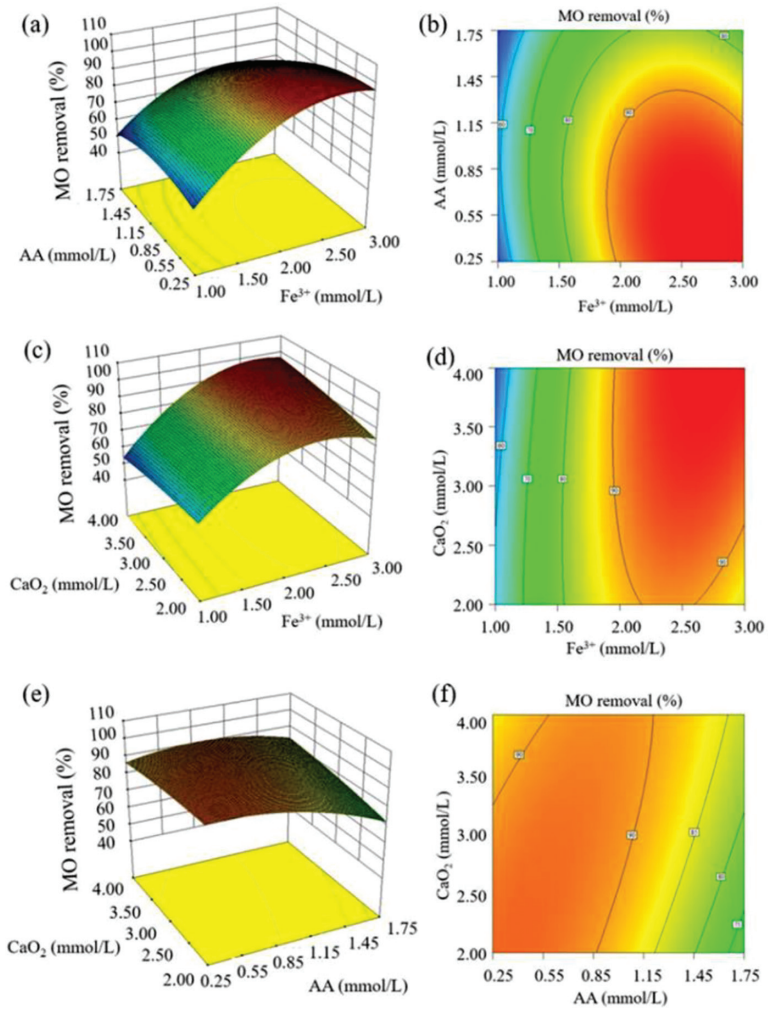

Fig. 2. Response surface plots of interaction for two independent variables: Fe^{3+} and AA (a and b), CaO_2 and Fe^{3+} (c and d), and CaO_2 and AA (e and f).

Fig. 1b shows the change of MO absorption peak (465 nm) with treatment time. The characteristic peak intensity decreased with the increase of time, which indicated that the azo bond of MO was attacked and cleaved by the active substances [38,39]. At the same time, the peak intensity at less than 300 nm increased gradually, proving that more small molecules were formed during the MO removal [40]. The mineralization of MO was verified by the TOC analysis. As show in Fig. 1c, the TOC removal enhanced with the treatment time, and reaches 19.40% after 120 min, proving that the dye molecular structure was decomposed into lesser organic matters and mineralized into H_2O and CO_2 under the synergistic process. The comparatively low TOC removal could be attributed to the addition of organic acid complexing agent, which would compete with the reactive species generated in the synergy and enhance the organic load of wastewater. Besides, the oxidation performance of Fe^{3+}/AA/CaO_2 for different organic dyes were determined (Fig. 1d). Other four dyes (Congo red (CGR), acid fuchsin (AF), methylene blue (MB), and reactive brilliant blue (KN-R)) were treated under the Fe^{3+}/AA/CaO_2 system with the identical conditions, and their decolorization efficiencies all were higher than 84.00% after 15 min reaction, certifying this coupling system has a good ability to treat various dye wastewaters.

Table S2 (Supporting information) lists the three levels and three variables full factor analysis of each experiment based on RSM results, including the experimental and predicted values of MO removal. According to the results and data analysis, the quadratic linear regression equation obtained by running Design-Expert 8.0.6 trial software was as follows [41,42]:

$$Y = 90.80 + 16.63X_1 - 5.88X_2 + 1.25X_3 - 4.05X_1X_2 + 4.75X_1X_3 + 4.25X_2X_3 - 15.4{X_1}^2 - 5.90{X_1}^2 - 1.15{X_3}^2 \quad (10)$$

Table S3 (Supporting information) displays the results of variance analysis. The *P*-value was less than 0.0001, indicating that the result was significant, and the 51.23 of *F*-value was a further proof of the significant model [43]. Meanwhile, due to the influence of interference error, only 0.01% chance would appear such a large *F*-value. The R^2 value indicates that the model is to what extent impact the variability of data. In this study, the R^2 value of quadratic linear regression model was 0.9850, demonstrating that 98.50% of the MO removal efficiency was affected by the independent variables, and only 1.50% of influence was unaffected by the model. ${R_{adj}}^2$ is optimized for R^2 by considering the covariates or predictors, which is more suitable to compare those models with various of arguments. The

value of R_{adj}^2 (0.9658) was close to that of R^2, ensuring the reliability of quadratic model. In addition, the signal to noise ratio of 20.199 showed that the result was feasible for this model [44].

Verification of model feasibility is a vital process, which is the indispensable way to evaluate whether the result is suitable. The linear distribution points of normal probability plots can prove the residuals obey normal distribution. As shown in Fig. S1a (Supporting information) the points were distributed on both sides of the straight line, proving it obeyed normal distribution. Also, the result suggested that the quadratic formula given by the model could well predict the effect of Fe^{3+}, AA and CaO_2 on the MO decolorization. Fig. S1b (Supporting information) presents the comparison of MO removal ratio for the predicted and experimental values. All the spots were dispersed around the regression curve, testifying that the simulated outcomes were consistent with the actual data. From Fig. S1c (Supporting information), the residuals were randomly distributed around 0 with the change of ± 3.0, indicating that the response of model was identical to the normal distribution. Fig. S1d (Supporting information) reveals the matching correlation for the residual and simulative values. The residual was a random distribution, manifesting that the change of original value was constant for the response value [44].

The response surface and contour could manifest the interaction of various factors on the decolorization of MO. Fig. 2a shows the effect of Fe^{3+} and AA concentrations on the MO removal. The dose of CaO_2 was fixed at 3 mmol/L. The decolorization of MO underwent an increase and decrease with the increscent AA amount (0.25 to 1.75 mmol/L). This is because the excessive AA would react with active substances. With the increase of Fe^{3+} concentration from 1 mmol/L to 3 mmol/L, the removal of MO also enhanced, proving that the Fe^{3+} was a crucial factor as a catalyst in this synergistic method. Fig. 2b confirmed that there was interaction between Fe^{3+} and AA, then the generated functions of complexation and reduction could improve the Fenton-like reaction and MO removal. Fig. 2c reveals the effect of Fe^{3+} and CaO_2 concentrations on the decolorization of MO. The concentration of AA kept constant. When AA was 1 mmol/L, the MO removal increased with the enhancing CaO_2 amount. This is due to the fact that the more oxidant added, the more active species would be produced in the system, benefiting the dye removal. Fig. 2d also verified the interrelationship between Fe^{3+} and CaO_2. Figs. 2e and f present the effect of AA and CaO_2 quantities on the MO elimination. The Fe^{3+} concentration remained at 2 mmol/L. With the decrease of AA dosage and the increase of CaO_2 amount, the MO decolorization was augmented. The result suggested that there was an optimum for the AA addition.

As the predesigned experiments were completed, Design-Expert 8.0.6 was applied to optimize parameters for the Fe^{3+}/AA/CaO_2 system. The simulation result indicated that the best MO decolorization was 99.30% under the optimal conditions of 2.76 mmol/L Fe^{3+}, 0.68 mmol/L AA and 4 mmol/L CaO_2. Furthermore, the proof test demonstrated that the elimination of MO could reach 98.90% under the same conditions. The experimental outcome was agreed well with the predicted value, attesting that the RSM model was reliable and its optimization was successful.

Owing to the significant influence of solution pH on the Fenton process, the MO removal in the Fe^{3+}/AA/CaO_2 was investigated at the different initial pH. Fig. 3a displays that the MO eliminations varied little when the wastewater pH changed from 3 to 11, and the decolorizations were all higher than 90%. The result demonstrated that the presented collaborative Fenton-like system could perform well in a wide range of pH.

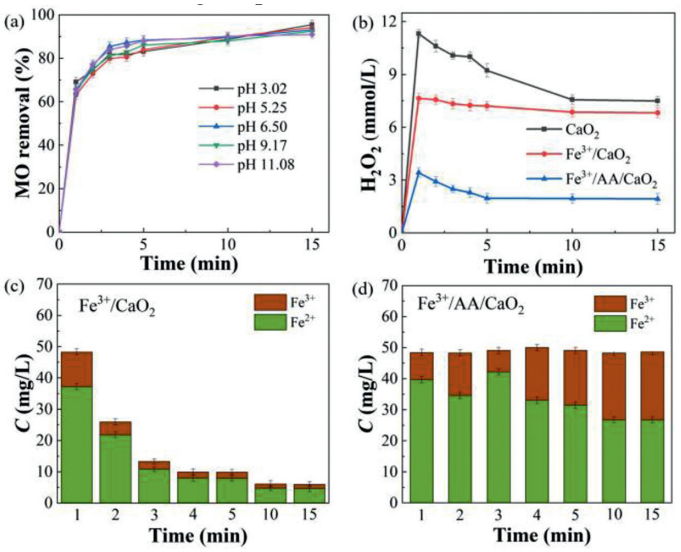

Fig. 3. (a) Effect of pH on MO removal in Fe^{3+}/AA/CaO_2. (b) H_2O_2 concentrations in different processes. Fe^{2+} and Fe^{3+} concentrations in Fe^{3+}/CaO_2 (c) and Fe^{3+}/AA/CaO_2 (d). Conditions: [MO] = 0.15 mmol/L, [Fe^{3+}] = 2 mmol/L, [AA] = 1 mmol/L, [CaO_2] = 3 mmol/L, initial pH 6.50.

Fig. 3b presents change of H_2O_2 concentration during the diverse processes. The H_2O_2 amounts all rose at the beginning and then declined with the time for the three experiments, and their sequence was: CaO_2 > Fe^{3+}/CaO_2 > Fe^{3+}/AA/CaO_2. The phenomena suggested that the addition of AA could be beneficial to improve the H_2O_2 decomposition.

The variations of Fe^{3+} and Fe^{2+} concentrations during the Fe^{3+}/CaO_2 and Fe^{3+}/AA/CaO_2 systems are shown in Figs. 3c and d, respectively. The total Fe ions content of Fe^{3+}/AA/CaO_2 remained constant, and which was decreased sharply with time in the Fe^{3+}/CaO_2. Besides, the Fe^{2+} concentration of the complexation system was obviously higher than that of Fe^{3+}/CaO_2. Above result verified the complexing function of AA, which could not only maintain the dissolved state for Fe^{3+} and Fe^{2+}, but also improve the remarkably promote the reduction of Fe^{3+} and reduce the iron sludge generation.

The reactive oxygen species masking experiment was employed to investigated the functions of various active species in the Fe^{3+}/AA/CaO_2 system (Fig. 4). TBA can effectively quench $^{\bullet}OH$, and the reaction rate constant is 6.0×10^8 L mol^{-1} s^{-1} [45,46]. BQ is commonly used as a scavenger of $O_2^{\bullet-}$, (9.6×10^8 L mol^{-1} s^{-1}), and L-histidine can mask $^1O_2$ and $^{\bullet}OH$ [47–49]. In Fig. 4a, the addition of TBA significantly inhibited the removal of MO, and the decolorization rate decreased from 93% to 55% as the TBA increased from 0 to 60 mmol/L. However, when the concentration of TBA was enhanced to 60 mmol/L, the suppression effect was obviously weakened. It could be concluded that excessive TBA could not completely confine the MO decolorization, and other active substances also were responsible for the elimination of MO. From Fig. 4b, while the amount of BQ was augmented from 0.1 mmol/L to 0.5 mmol/L, the MO decolorization was declined from 87% to 59%, showing that $O_2^{\bullet-}$ was also played a non-ignorable role for the dye decontamination. Fig. 4c displays that the scavenging effect was augmented with the increase of L-histidine. When the concentration of L-histidine was enhanced to 4 mmol/L, the MO decolorization declined to 25%, demonstrating that $^1O_2$ was also

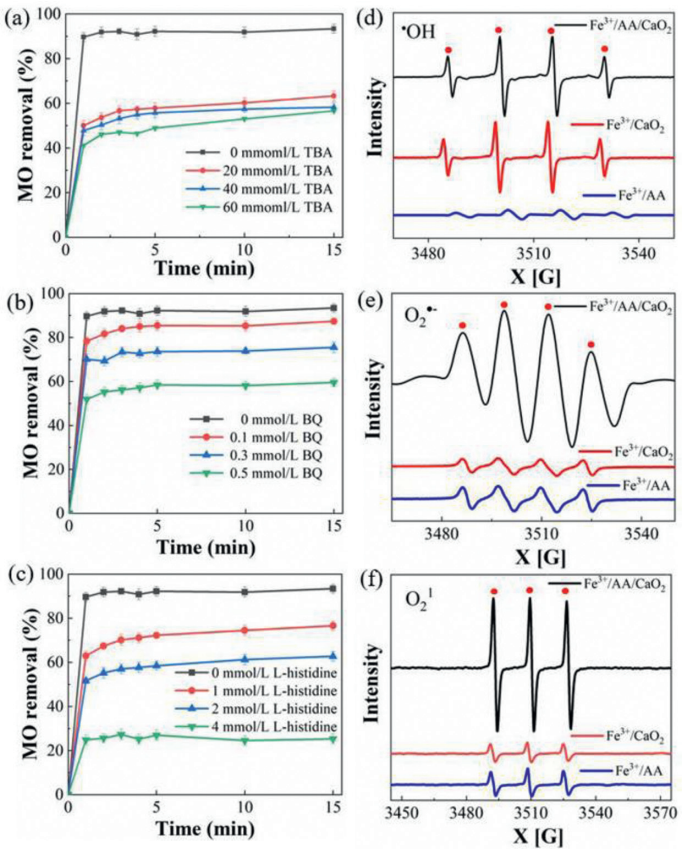

Fig. 4. Effect of different scavengers on MO removal in $Fe^{3+}/AA/CaO_2$: (a) TBA, (b) BQ, (c) L-histidine. ESR spectra for •OH (d), $^1O_2$ (e), and $O_2^{\bullet-}$ (f).

an essential reactive species in this Fenton-like system. In addition, the ESR analysis was employed to further confirm the existences of these active species. The typical signals for •OH, $O_2^{\bullet-}$ and $^1O_2$ were detected in the spectrum of Figs. 4d–f, respectively. Obviously, these peak intensities for the $Fe^{3+}/AA/CaO_2$ was higher than those of Fe^{3+}/CaO_2 and Fe^{3+}/AA, corroborating that the generations of these reactive species in the collaborative system. More importantly, the ESR results were in accordance with the scavenging tests.

Moreover, to explore the role of Fe^{4+} in this oxidative process, the Fe^{4+} amounts were measured by DMSO oxidation method. From Fig. S2 (Supporting information), the difference for the consumptions of DMSO was not significant in the Fe^{3+}/CaO_2 and $Fe^{3+}/AA/CaO_2$ systems. Furthermore, the formations of dimethyl sulfone ($DMSO_2$) were quite small and comparative, indicating that the Fe^{4+} productions were tiny during the two processes. Besides, the little decrease of the DMSO could be attributed to the attack of •OH radical [33]. These results proved that the Fe^{4+} was not the dominant active species in the $Fe^{3+}/AA/CaO_2$.

In this work, a Fenton-like system using CaO_2 as the oxidant coupled with AA chelated Fe^{3+} was proposed to effectively remove various organic dyes in water. The $Fe^{3+}/AA/CaO_2$ process could significantly improve the MO decolorization compared with other control systems. By the RSM optimization, the mutual effect of operation conditions (concentrations of Fe^{3+}, AA and CaO_2) was explored, and the optimal parameters were obtained (2.76 mmol/L Fe^{3+}, 0.68 mmol/L AA and 4 mmol/L CaO_2). Using the optimized parameters, the elimination of MO could reach 98.90% in the proof experiment, which was agreed well with the simulated result (99.30%). The complexation process could perform well in a wide range of pH (3–11), improving the H_2O_2 decomposition, and promoting the dissolution and cycle of Fe^{3+}/Fe^{2+}. The quenching test demonstrated that •OH, $O_2^{\bullet-}$ and $^1O_2$ were all responsible for the dye removal, and the ESR analysis certified the existence of these reactive species in the collaborative system. This work was fundamental to provide an improved and optimized method for Fenton-like technique.

Declaration of competing interest

The authors declare that they have no known competing financial interests or personal relationships that could have appeared to influence the work reported in this paper.

Acknowledgment

The authors thank the financial support from the Natural Science Foundation of China (No. 51908485), the Natural Science Foundation of Hebei province (Nos. E2020203185, B2020203033, B2018203331), and the University Science and Technology Program Project of Hebei Provincial Department of Education (No. QN2020143).

Supplementary materials

Supplementary material associated with this article can be found, in the online version, at doi:10.1016/j.cclet.2021.04.050.

References

[1] H. Zhang, Q. Ji, L. Lai, et al., Chin. Chem. Lett. 30 (2019) 1129–1132.
[2] Z. Wang, X. Teng, M. Xie, et al., Chin. Chem. Lett. 31 (2020) 2864–2870.
[3] M. Du, Q. Yi, J. Ji, et al., Chin. Chem. Lett. 31 (2020) 2803–2808.
[4] I.A. Ike, T. Karanfil, J. Cho, et al., Water Res. 164 (2019) 114929.
[5] D. Yuan, M. Sun, S. Tang, et al., Chin. Chem. Lett. 31 (2020) 547–550.
[6] J. Chen, J. Zhan, Y. Zhang, et al., Chin. Chem. Lett. 30 (2019) 735–738.
[7] Y. Li, W. Xiang, T. Zhou, et al., Chin. Chem. Lett. 31 (2020) 2757–2761.
[8] K. Wei, X. Cao, W. Gu, et al., Environ. Sci. Technol. 53 (2019) 6917–6926.
[9] I. Benhamed, L. Barthe, R. Kessas, et al., Appl. Catal. B: Environ. 187 (2016) 228–237.
[10] H. Guo, D. Li, Z. Li, et al., Sep. Purif. Technol. (2021) 118543.
[11] J. Li, Y. Li, Z. Xiong, et al., Chin. Chem. Lett. 30 (2019) 2139–2146.
[12] S. Tang, M. Zhao, D. Yuan, et al., Sep. Purif. Technol. 255 (2021) 117690.
[13] D. Yuan, C. Zhang, S. Tang, et al., Water Res. 163 (2019) 114861.
[14] H. Guo, Z. Li, Z. Xie, et al., Vacuum 185 (2021) 110022.
[15] C. Shan, H. Liu, M. Hua, et al., Environ. Sci. Technol. 54 (2020) 5893–5901.
[16] M. Gągol, A. Przyjazny, G. Boczkaj, Chem. Eng. J. 338 (2018) 599–627.
[17] Y. Zhu, R. Zhu, Y. Xi, et al., Appl. Catal. B: Environ. 255 (2019) 117739.
[18] X. Xu, W. Chen, S. Zong, et al., Chem. Eng. J. 373 (2019) 140–149.
[19] H. Luo, Y. Cheng, Y. Zeng, et al., Sci. Total Environ. 732 (2020) 139335.
[20] B. Shen, C. Dong, J. Ji, et al., Chin. Chem. Lett. 30 (2019) 2205–2210.
[21] D. Yuan, C. Zhang, S. Tang, et al., Sci. Total Environ. 727 (2020) 138773.
[22] Z. Ouyang, C. Yang, J. He, et al., Chem. Eng. J. 402 (2020) 126122.
[23] Z. Li, L. Wang, Y. Liu, et al., Water Res. 168 (2020) 115093.
[24] Amina, X. Si, K. Wu, et al., Chem. Eng. J. 353 (2018) 80–91.
[25] W. Wang, Y. Li, L. Li, et al., Int J. Electrochem. Sci. (2020) 11709–11722.
[26] M. Cao, Y. Hou, E. Zhang, et al., Chemosphere 229 (2019) 200–205.
[27] N. Dulova, E. Kattel, M. Trapido, Chem. Eng. J. 318 (2017) 254–263.
[28] S. Hadi, E. Taheri, M.M. Amin, et al., J. Environ. Manage. 268 (2020) 110678.
[29] Y. Zhou, M. Huang, X. Wang, et al., Chemosphere 253 (2020) 126662.
[30] Z. Sun, S. Li, H. Ding, et al., Chemosphere 241 (2020) 125125.
[31] S. Tang, D. Yuan, Y. Rao, et al., J. Hazard. Mater. 366 (2019) 669–676.
[32] S. Tang, Z. Wang, D. Yuan, et al., J. Clean. Prod. (2020) 122253.
[33] H. Bataineh, O. Pestovsky, A. Bakac, Chem. Sci. 3 (2012) 1594–1599.
[34] C. Wang, Y. Liu, T. Zhou, et al., Chin. Chem. Lett. 30 (2019) 2231–2235.
[35] M. Huang, W. Xiang, C. Wang, et al., Chin. Chem. Lett. 31 (2020) 2769–2773.
[36] X. Wang, Y. Du, H. Liu, et al., RSC Adv. 8 (2018) 12791–12798.
[37] W. Xiang, M. Huang, Y. Wang, et al., Chin. Chem. Lett. 31 (2020) 2831–2834.
[38] W. Szeto, J. Li, H. Huang, et al., Chem. Eng. Sci. 177 (2018) 380–390.
[39] X. Feng, Q. Li, K. Wang, ACS Appl. Mater. Interfaces 13 (2021) 400–410.
[40] H. Han, C. Shi, L. Yuan, et al., Appl. Energy 204 (2017) 382–389.

[41] K. Wang, C. Liu, J. Sun, et al., Complexity 2021 (2021) 8816250.
[42] K. Wang, W. Wang, L. Wang, et al., Energies 13 (2020) 5297.
[43] T. Wang, Y. Zhou, S. Cao, et al., Ecotoxcol. Environ. Saf. 172 (2019) 334–340.
[44] H. Li, Y. Gong, Q. Huang, et al., Ind. Eng. Chem. Res. 52 (2013) 15560–15567.
[45] S. Tang, M. Zhao, D. Yuan, et al., Chemosphere 268 (2021) 129315.
[46] D. Yuan, M. Sun, M. Zhao, et al., Int. J. Electrochem. Sci. 15 (2020) 8761–8770.
[47] J. Wang, S. Wang, Chem. Eng. J. 401 (2020) 126158.
[48] Z. Wu, K. Yin, J. Wu, et al., Nanoscale 13 (2021) 2209–2226.
[49] J. Wu, K. Yin, S. Xiao, et al., Adv. Mater. Interfaces 8 (2021) 2001610.